Scientific paper

Phase Equilibria in the Tl_4PbTe_3-Tl_9SmTe_6-Tl_9BiTe_6 Section of the Tl-Pb-Bi-Sm-Te System

Samira Zakir Imamaliyeva,[1,*] Alakbarzade Ganira Ilgar,[2] Mahmudova Matanat Aydin,[3] Amiraslanov Imameddin Rajabali[3] and Mahammad Baba Babanly[1]

[1] *Institute of Catalysis and Inorganic Chemistry named after acad. M. Nagiyev, Azerbaijan National Academy of Sciences, 113, H. Javid. ave., AZ-1143, Baku, Azerbaijan*

[2] *Azerbaijan State Oil and Industry University, 16/21, Azadlig Ave., AZ-1010, Baku, Azerbaijan*

[3] *Physics Institute, Azerbaijan National Academy of Sciences, 131, H. Javid ave., Az-1143, Baku, Azerbaijan*

* *Corresponding author: E-mail: samira9597a@gmail.com*

Received: 04-12-2017

Abstract

Phase equilibria in the section Tl_4PbTe_3-Tl_9SmTe_6-Tl_9BiTe_6 of the Tl-Pb-Bi-Sm-Te system were determined by combination of differential thermal analysis, powder X-ray diffraction methods as well as microhardness measurements. The phase diagrams of the boundary systems Tl_4PbTe_3-Tl_9SmTe_6, Tl_9SmTe_6-Tl_9BiTe_6, isothermal section at 820 and 840 K, some isopleth sections and as well as liquidus and solidus surfaces projections, were plotted. Unlimited solid solutions, which crystallize in Tl_5Te_3 structure type were found in the system at the solidus temperatures and below.

Keywords: Thallium-lead telluride; thallium-samarium tellurides; thallium-bismuth tellurides; phase equilibria; liquidus and solidus surfaces; solid solutions

1. Introduction

Complex chalcogenides based materials of great interest for many years due to their functional properties such as optic, photoelectric, magnet, thermoelectric et al.[1–3] Some of these materials exhibit properties of topological insulators and can use in spintronic devices.[4–6] Furthermore, a number of papers present the results of the study of interactions of the rare-earth elements with heavy elements chalcogenides.[7–9]

Tl_5Te_3 compound crystallizes in tetragonal structure (Sp.gr.I4/mcm, a = 8.930; c = 12.598 Å), [10,11] and has a number of ternary substitutional analogs of $Tl_4A^{IV}Te_3$ and $Tl_9B^{V}Te_6$ -type (A^{IV}-Sn, Pb; B^{V}-Sb, Bi),[12–14] which also possess a good thermoelectric performance.[15,16] Moreover, authors[17] found the Dirac-like surface states in the $[Tl_4]TlTe_3$ (Tl_5Te_3) and its non-superconducting tin-doped derivative $[Tl_4](Tl_{1-x}Sn_x)Te_3$.

A new thallium lanthanide tellurides of Tl_9LnTe_6 -type (Ln-Ce, Nd, Sm, Gd, Tb, Tm) were found to be a new structural analog of Tl_5Te_3.[18,19] H. Kleinke and co-workers [20–22] confirmed the results of the studies,[18,19] and determined the thermoelectric and magnetic properties for a number Tl_9LnTe_6-type compounds.

The development of the novel preparative methods for direct synthesis of functional materials requires to provide an accurate study of phase relations and plot the phase diagram.

Early, we presented the results of a study of phase relations for a number of systems including the Tl_5Te_3 compound or its structural analogs.[23–25] The formation of unlimited solid solutions was shown for these systems.

In this paper, we continue to study similar systems and present the experimental results on phase equilibria in the Tl_4PbTe_3-Tl_9SmTe_6-Tl_9BiTe_6 section of the Tl-Pb-Bi-Sm-Te system.

The initial compounds of above-mentioned system have been studied in a number of papers. Tl_4PbTe_3 and Tl_9BiTe_6 melt congruently at 893 K,[26] and 830 K,[14] respectively, while Tl_9SmTe_6 is formed incongruently at 755 K.[25] The tetragonal lattice constants of Tl_4PbTe_3, Tl_9SmTe_6, and Tl_9BiTe_6 are following: a = 8.841, c =

13.056Å, z = 4[27]; a = 8.888; c = 13.013 Å, z = 2[28]; a = 8.855, c = 13.048 Å, z = 2.[25]

According to Ref.[26], the boundary system Tl_4PbTe_3-Tl_9BiTe_6 is quasi binary and characterized by the formation of unlimited solid solutions (δ) with Tl_5Te_3-structure.

2. Experimental

2. 1. Materials and Syntheses

The following reagents were used as starting components: thallium (granules, 99.999%), lead (ingot, 99.99%), samarium (powder, 99.9%), bismuth (granules, 99.999%), and tellurium (broken ingots 99.999%).

We used protective gloves at all times when working with thallium because thallium and its compounds are highly toxic and contact with skin is dangerous.

Stoichiometric amounts of the starting components were weighed with accuracy ±0.0001 g. Then they were put into silica tubes of about 20 cm in length and diameter about 1.5 cm and sealed under a vacuum of 10^{-2} Pa. Tl_4PbTe_3 and Tl_9BiTe_6 were synthesized by heating in a resistance furnace at 920 K followed by cooling in the switched-off furnace.

In the case of Tl_9SmTe_6, the ampoule was graphitized using pyrolysis of toluene in order to prevent the reaction of samarium with quartz. Taking into account the results of the work[26], the intermediate ingot of Tl_9SmTe_6 was powdered in an agate mortar, carefully mixed, pressed into a pellet and annealed at 700 K within ~700 h.

The resulting ingots were homogeneous polycrystals alloys that were established by the differential thermal analysis (DTA) and X-ray diffraction (XRD).

The alloys of the Tl_4PbTe_3-Tl_9SmTe_6-Tl_9BiTe_6 system were prepared by melting of previously synthesized ternary compounds. After synthesis the samples containing >60% Tl_9SmTe_6 were powdered, carefully mixed, pressed into pellets and annealed at 700 K during ~ 800 h in order to complete the homogenization. The total mass of each ingot is about 1 g.

2. 2. Methods

DTA and XRD analyses, as well as microhardness measurements, were used to analyze the samples of the investigated system.

The phase transformation temperatures were determined using a NETZSCH 404 F1 Pegasus differential scanning calorimeter within room temperature and ~1400 K at a heating rate of 10 K · min^{-1} and accuracy about ±2 K. The phase identification was performed using a Bruker D8 diffractometer utilizing CuK_α radiation. The powder diagrams of the ground samples were collected at room temperature in the 2θ range of 6–75°. The unit cell parameters of intermediate alloys were calculated by indexing of powder patterns using Topas V3.0 software. An accuracy of the crystal lattice parameters is shown in parentheses (Table). Microhardness measurements were done with a microhardness tester PMT-3, the typical loading being 20 g and accuracy about 20 MPa.

3. Results and Discussion

The Tl_4PbTe_3-Tl_9SmTe_6-Tl_9BiTe_6 section was plotted based on combined analysis of experimental results and literature data on boundary system Tl_4PbTe_3-Tl_9BiTe_6[26] (Fig. 1–6).

Table 1. Experimental data of the DTA, microhardness measurements and parameters of tetragonal lattice for the alloys of the Tl_4PbTe_3-Tl_9SmTe_6 and Tl_9BiTe_6-Tl_9SmTe_6 sections of the Tl-Pb-Bi-Sm-Te system

Solid phase compositions	Thermal effects, K	Microhardness, MPa	Tetragonal lattice parameters, Å	
			a	*c*
Tl_4PbTe_3	893	1120	8.8409(5)	13.0556(6)
$Tl_{8.2}Pb_{1.6}Sm_{0.2}Te_6$	845–875	1160	8.8504(4)	13.0482(9)
$Tl_{8.4}Pb_{1.2}Sm_{0.4}Te_6$	820–850	1180	8.8602(5)	13.0387(8)
$Tl_{8.5}Pb_{1.0}Sm_{0.5}Te_6$	817–845	–	8.8645(6)	13.0343(9)
$Tl_{8.6}Pb_{0.8}Sm_{0.6}Te_6$	790–830	1150	8.8702(6)	13.0298(9)
$Tl_{8.8}Pb_{0.4}Sm_{0.8}Te_6$	775–800; 1190	1140	8.8788(5)	13.0280(9)
$Tl_{8.9}Pb_{0.2}Sm_{0.9}Te_6$	760–775; 1155	–	–	–
Tl_9SmTe_6	755; 1180	1080	8.8882(5)	13.0132(7)
$Tl_9Bi_{0,1}Sm_{0,9}Te_6$	760; 1150	–	–	–
$Tl_9Bi_{0,2}Sm_{0,8}Te_6$	765–775; 1095	1120	8.8810(4)	13.0201(7)
$Tl_9Bi_{0,4}Sm_{0,6}Te_6$	770–790	1140	8.8741(5)	13.0279(8)
$Tl_9Bi_{0,5}Sm_{05}Te_6$	780–800	–	8.8710(5)	13.0301(8)
$Tl_9Bi_{0,6}Sm_{0,4}Te_6$	785–810	1110	8.8673(5)	13.0340(9)
$Tl_9Bi_{0,8}Sm_{0,2}Te_6$	810–820	1070	8.8614(5)	13.0410(8)
Tl_9BiTe_6	830	980	8.8545(4)	13.0476(7)

The Table presents the results of DTA, microhardness measurements, and parameters of the tetragonal lattice for starting compounds and some intermediate alloys.

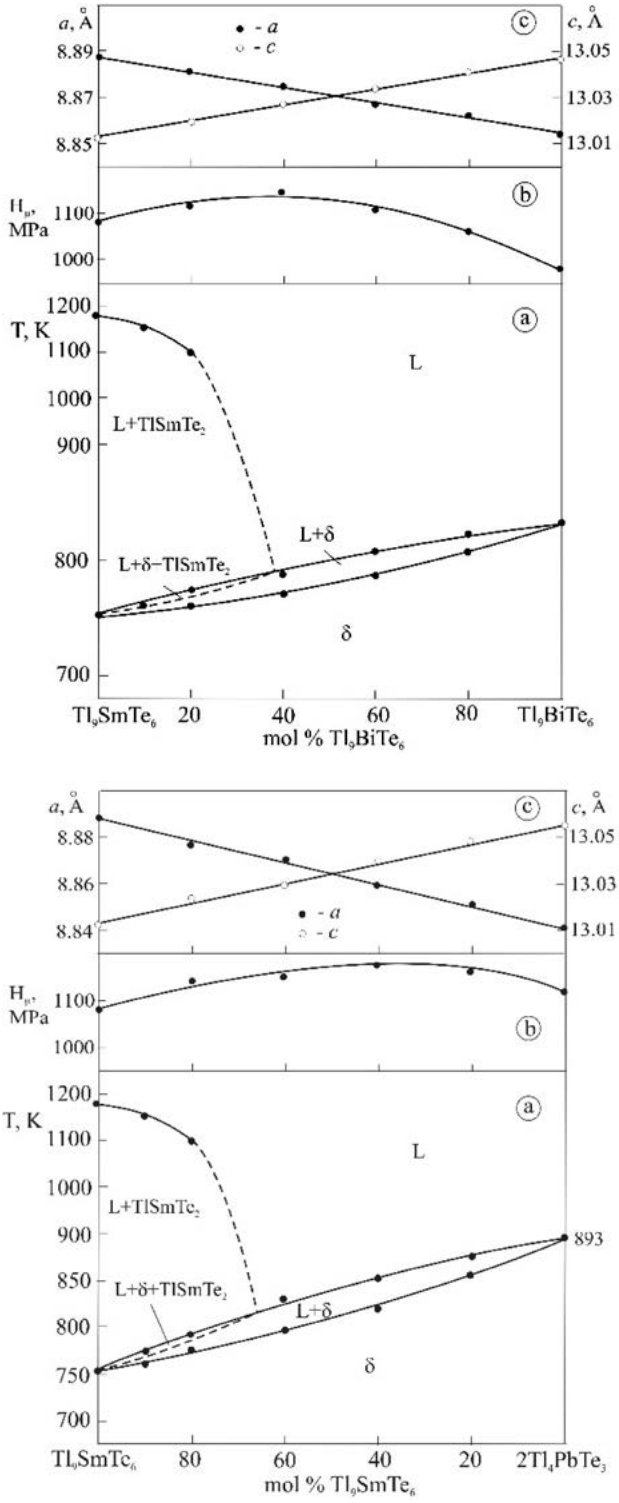

Fig. 1. Polythermal sections (a), concentration dependencies of microhardness (b), and lattice parameters (c) for the alloys of the Tl_9SmTe_6-Tl_9BiTe_6 and Tl_4PbTe_3-Tl_9SmTe_6 sections of the Tl-Pb-Bi-Sm-Te system.

Phase diagrams and the composition dependences of properties are plotted based on these data.

Tl_4PbTe_3-Tl_9SmTe_6 and Tl_9BiTe_6-Tl_9SmTe_6 sections (Fig. 1) are characterized by the formation of unlimited solid solutions (δ) with Tl_5Te_3-structure. But, they are non-quasi-binary sections of the Tl-Pb-Sm-Te and Tl-Bi-Sm-Te quaternary systems due to the peritectic character of melting of Tl_9SmTe_6. As the result, the crystallization of $TlSmTe_2$ compound occurs in a wide composition interval which leads to the formation of two-phase L+$TlSmTe_2$ and three-phase L+$TlSmTe_2$+δ areas. The L+$TlSmTe_2$+δ area is shown by a dotted line because not fixed experimentally due to a narrow interval of temperatures.

In order to determine the phase constituents, polished surfaces of the intermediate samples were visually observed under the microscope of microhardness meter. The microhardness curves have a flat maximum which is typical for systems with unlimited solid solutions (Fig. 1b). [29]

The XRD powder patterns for some alloys of the Tl_4PbTe_3-Tl_9SmTe_6 and Tl_9BiTe_6-Tl_9SmTe_6 sections are presented in Fig. 2. Powder diffraction patterns of Tl_4PbTe_3, Tl_9SmTe_6, and Tl_9BiTe_6 as well as intermediate alloys are single-phase and have the diffraction patterns qualitatively similar to Tl_5Te_3 with slight reflections displacement from one compound to another. For example, we present the powder diffraction patterns of alloy with composition 20, 50 and 80 mol% Tl_9SmTe_6 for both systems. Parameters of the tetragonal lattice of solid solutions obey the Vegard's law (Table, Fig. 1c).

Isopleth sections of the Tl_4PbTe_3-Tl_9SmTe_6-Tl_9BiTe_6 system (Fig. 3).

In order to construct a complete T-x-y diagram and to refine the boundaries of areas of primary crystallization of δ-phase and $TlSmTe_2$, we constructed some isopleth sections. Figs.3a–c present the isopleth sections Tl_9SmTe_6-[A], Tl_9BiTe_6-[B] and Tl_4PbTe_3-[C] of the Tl_4PbTe_3-Tl_9SmTe_6-Tl_9BiTe_6 system, where A, B, and C are equimolar alloys from the respective boundary system as shown in Fig. 4.

Along the Tl_9SmTe_6-[A] section, the δ-phase crystallizes in the composition area <60 mol% Tl_9SmTe_6. In the Tl_9SmTe_6- rich interval the $TlSmTe_2$ primary crystallizes, then a monovariant peritectic process L+$TlSmTe_2$ ↔ δ takes place (Fig. 3a).

Over the entire compositions range of the Tl_9BiTe_6-[B] and Tl_4PbTe_3-[C] sections, crystallization of the δ-phase occurs from the melt (Fig. 3b,c,).

The XRD powder patterns for selective alloys on polythermal sections confirmed continuous solid solutions with the Tl_5Te_3- structure.

The liquidus and solidus surfaces projections (Fig. 4)

Projection of liquidus of Tl_4PbTe_3-Tl_9SmTe_6-Tl_9BiTe_6 section consists of two fields of the primary crystallization of $TlSmTe_2$ and δ- solid solutions. These fields are separated by a monovariant peritectic curve L+$TlSmTe_2$ ↔ δ (ab curve). The solidus projection (dashed lines) con-

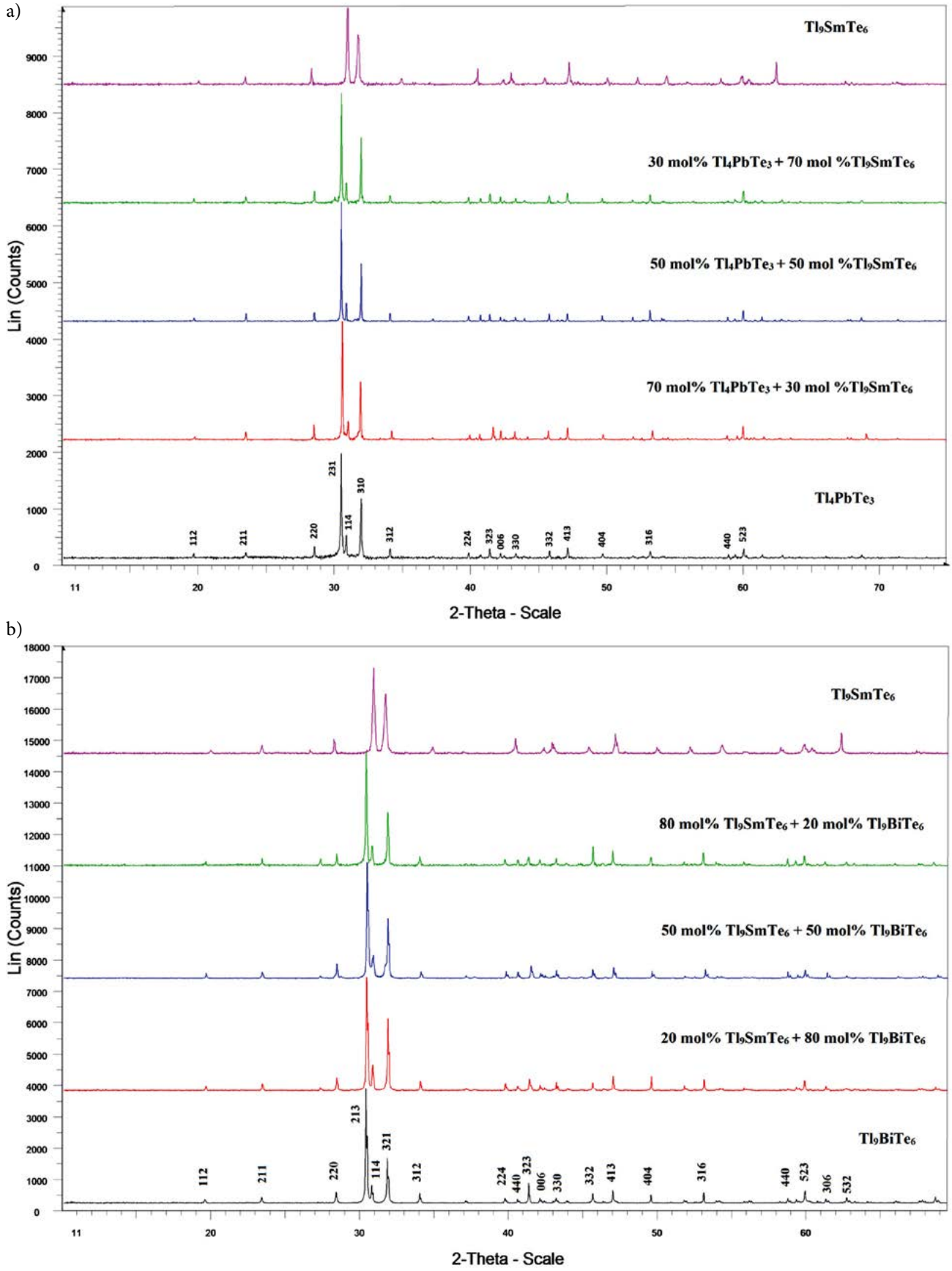

Fig. 2. XRD powder patterns for starting compounds and some alloys of the Tl_4PbTe_3-Tl_9SmTe_6 (a) and Tl_9SmTe_6-Tl_9BiTe_6 (b) systems.

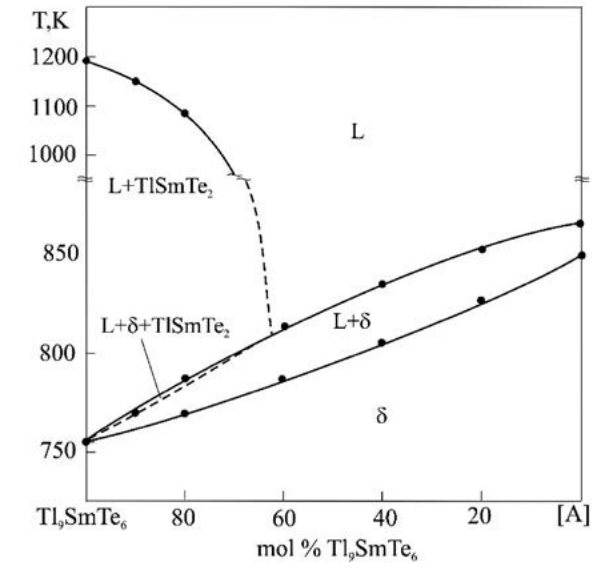

a)

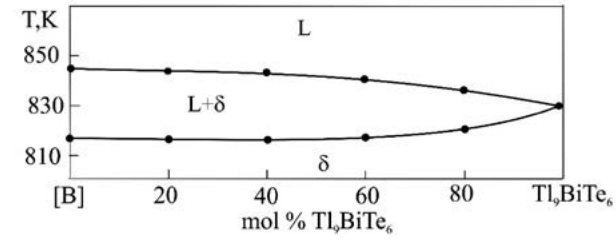

b)

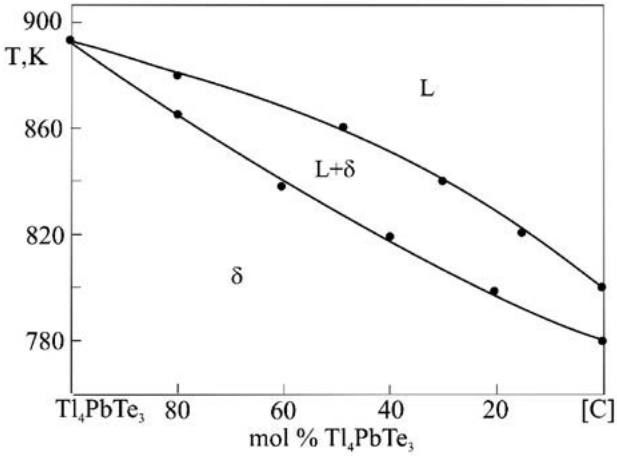

c)

Fig. 3. Polythermal sections Tl_9SmTe_6-[A], Tl_9BiTe_6-[B] and Tl_4PbTe_3-[C] of the phase diagram of the Tl_4PbTe_3-Tl_9SmTe_6-Tl_9BiTe_6 section of the Tl-Pb-Bi-Sm-Te system. A, B, and C are equimolar alloys from the respective boundary system as shown in Fig. 4.

sist of one surface corresponding to the completion of the crystallization of the δ-phase.

Isothermal sections at 820 and 840 K of the Tl_4PbTe_3-Tl_9SmTe_6-Tl_9BiTe_6 section (Fig. 5) are consists of areas of L-, $TlSmTe_2$ and δ- phases. In alloys <60 mol% Tl_9SmTe_6 in the two-phase L+δ region the directions of the

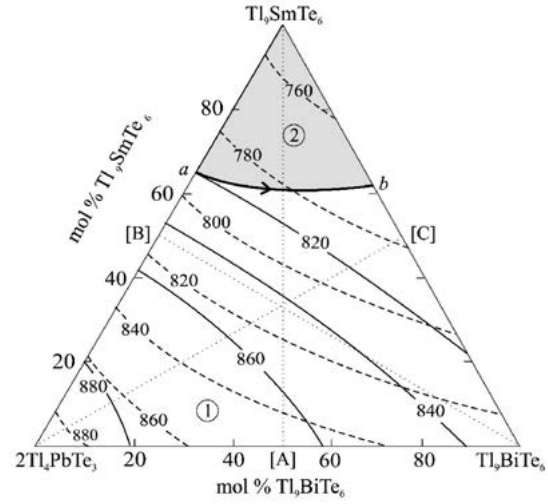

Fig. 4. The liquidus and solidus surfaces projections Tl_4PbTe_3-Tl_9SmTe_6-Tl_9BiTe_6 section of the Tl-Pb-Bi-Sm-Te system. The investigated sections are shown by dash-dot lines. A, B and C are equimolar compositions of the boundary systems. Primary crystallization phases: 1-δ; 2-$TlSmTe_2$

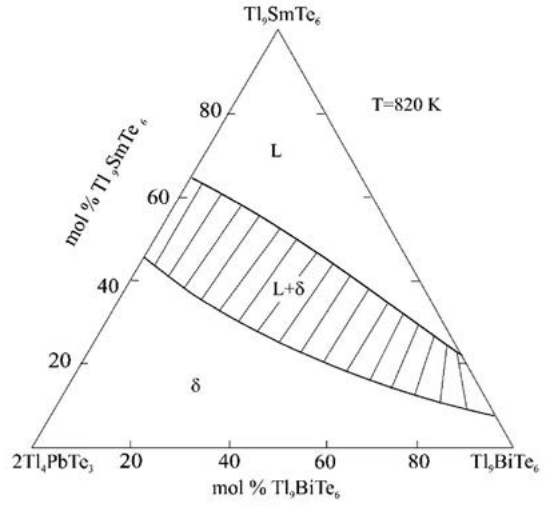

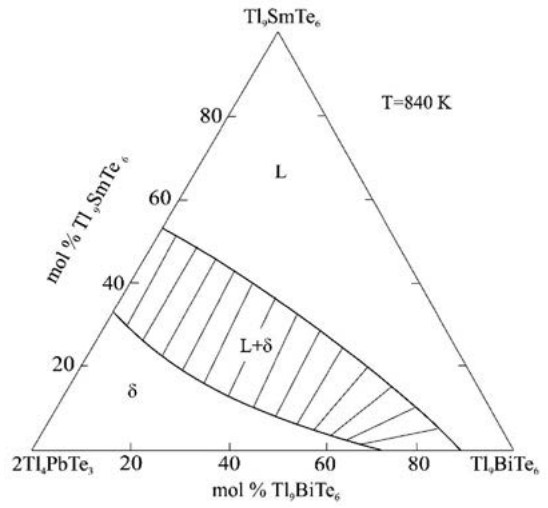

Fig. 5. Isothermal sections at 820 and 840 K in the Tl_4PbTe_3-Tl_9SmTe_6-Tl_9BiTe_6 section of the Tl-Pb-Bi-Sm-Te system.

connodes are on the studied composition plane. It should be noted that comparison of the isopleth sections (Fig. 3) and isothermal sections (Fig. 5) shows that the directions of the connodes in the two-phase region L+δ deviate from the *T–x* plane and constantly vary with temperature. Isothermal sections at 820 and 840 K clearly confirm this.

4. Conclusion

A complete phase diagram of the Tl-Pb-Bi-Sm-Te system in the Tl_4PbTe_3-Tl_9SmTe_6-Tl_9BiTe_6 composition interval is plotted. Unlimited solubility of components in the solid state is found in the studied section. Obtained experimental results can be used for choosing the composition of solution-melt for the growth of the high-quality crystals of δ- phase which is of interest as thermoelectric material.

5. Acknowledgment

The work has been carried out within the framework of the international joint research laboratory "Advanced Materials for Spintronics and Quantum Computing" (AMSQC) established between Institute of Catalysis and Inorganic Chemistry of ANAS (Azerbaijan) and Donostia International Physics Center (Basque Country, Spain).

6. References

1. Applications of Chalcogenides: S, Se, and Te, ed. by Gurinder Kaur Ahluwalia, Springer, **2016**.
2. A. V. Shevelkov, *Russ. Chem. Rev*, **2008**, *77*, 1–19 **DOI:**10.1070/RC2008v077n01ABEH003746
3. M. G. Kanatzidis, in T. M. Tritt (ed.), Semiconductors and semimetals. San Diego; San Francisco; N. Y.; Boston; London; Sydney; Tokyo: Academ. Press. **2001**, *69*, 51–98.
4. N. Singh and U. Schwingenschlogl, *Phys. Status Solidi RRL*. **2014**, 8, 805–808. **DOI:**10.1002/pssr.201409110
5. Y. L. Chen, Z. K .Liu, J. G. Analytis, J. H. Chu, H. J. Zhang, B. H. Yan et al., *Phys Rev Lett*., **2010**, *105*, 266–401. **DOI:**10.1103/PhysRevLett.105.266401
6. S. V. Eremeev, Yu. M. Koroteev, E. V. Chulkov, *JETP Lett.,* **2010**, *92*, 161–165. **DOI:**10.1134/S0021364010150087
7. C. Zhou, L. Li, *J. Phys. Chem. Solids*, **2015**, *85*, 239–244. **DOI:**10.1016/j.jpcs.2015.05.021
8. B. Yan, H-J. Zhang, C-X. Liu, X-L. Qi, T. Frauenheim and S-C. Zhang, *Phys. Rev. B*. **2010**, *82*, 161–108(R)-7
9. O. V. Andreev, V. G. Bamburov, L. N. Monina, I. A. Razumkova, A. V. Ruseikina, O. Yu. Mitroshin, V. O. Andreev, Phase equilibria in the sulfide systems of the 3d, 4f-elements. Ekaterinburg: Editorial Publication Department of the UR RAS, **2015**
10. I. Schewe, P. Böttcher, H. G. Schnering, *Z. Kristallogr.* **1989**, *Bd188*, 287–298. **DOI:**10.1524/zkri.1989.188.3-4.287
11. R. Cerny, J. Joubert, Y. Filinchuk, Y. Feutelais, *Acta Crystallogr*. C., **2002**, *58*, 163.
12. A. A. Gotuk, M. B. Babanly, A. A. Kuliev, *Inorg. Mater.* **1979**, *15*, 1062–1067.
13. M. B. Babanly, A. Azizulla, A. A. Kuliev, *Russ. J. Inorg. Chem*. **1985**, *30*, 1051–1059.
14. M. B. Babanly, A. Azizulla, A. A. Kuliev, *Russ. J. Inorg. Chem*. **1985**, *30*, 2356–2359.
15. B. Wolfing, C. Kloc, J. Teubner, E. Bucher, *Phys. Rev. Let*. **2001**, *36*, 4350–4353. **DOI:**10.1103/PhysRevLett.86.4350
16. Q. Guo, M. Chan, B. A. Kuropatwa, H. Kleinke, *J. Appl. Phys*., 2014, *116*, 183702/1–9
17. K. E. Arpino, D. C. Wallace, Y. F. Nie, T. Birol, P. D. C. King, S. Chatterjee, M. Uchida, S. M. Koohpayeh, J.-J. Wen, K. Page, C. J. Fennie, K. M. Shen, and T. M. McQueen, *Phys. Rev. Lett.* (PRL). **2014**, *112*, 017002–5. **DOI:**10.1103/PhysRevLett.112.017002
18. S. Z. Imamalieva, F. M. Sadygov, M. B. Babanly, *Inorg. Mater.* **2008**, *44*, 935–938. **DOI:**10.1134/S0020168508090070
19. M. B. Babanly, S. Z. Imamaliyeva, D. M. Babanly, *Azerb. Chem.* J. **2009**, *2*, 121–125.
20. S. Bangarigadu-Sanasy, C. R. Sankar, P. Schlender, H. Kleinke, *J. Alloys Compd*. **2013**, *549*, 126–134. **DOI:**10.1016/j.jallcom.2012.09.023
21. S. Bangarigadu-Sanasy, C. R. Sankar, P. A. Dube, J. E. Greedan, H. Kleinke, *J.Alloys. Compd.* **2014**, *589*, 389–392. **DOI:**10.1016/j.jallcom.2013.11.229
22. Q. Guo, H. Kleinke, *J. Alloys. Compd.* **2015**, *630*, 37–42. **DOI:**10.1016/j.jallcom.2015.01.025
23. S. Z. Imamaliyeva, T. M. Gasanly, V. A. Gasymov, M. B. Babanly, *Acta Chim. Slov.*, **2017**, *64,* 221–226. **DOI:**10.17344/acsi.2017.3207
24. S. Z. Imamaliyeva, I. F. Mekhdiyeva, V. A. Gasymov, M. B. Babanly, *Mater.Res.*, **2017**, *20*, 1057–1062. **DOI:**10.1590/1980-5373-mr-2016-0894
25. S. Z. Imamaliyeva, V. A. Gasymov, M. B. Babanly, *Chemist*, **2017**, *90*, 1–6.
26. M. B. Babanly, G. B. Dashdiyeva, F. N. Guseinov, *Chem . Probl.*, **2008**, *1*, 69–72.
27. S. Bradtmöller, P. Böttcher, *Z. anorg. allg. chem*., **1993**, *619*, 1155–1160. **DOI:**10.1002/zaac.19936190702
28. T. Doert, P. Böttcher, *Z. Kristallogr.,* **1994**, *209*, 95.
29. V. M. Glazov, V. N. Vigdorovich, *Mikrotverdost' metallov i poluprovodnikov* (Microhardness of Metals and Semiconductors), Moscow: Metallurgiya, **1969.**

Povzetek

V sistemu Tl-Pb-Bi-Sm-Te smo preučevali fazna ravnotežja dela Tl_4PbTe_3-Tl_9SmTe_6-Tl_9BiTe_6 s termično analizo, rentgensko praškovno difrakcijo in meritvami mikrotrdote. Pripravili smo fazne diagrame sistemov Tl_4PbTe_3-Tl_9SmTe_6, Tl_9SmTe_6-Tl_9BiTe_6, izotermične krivulje pri 820 K in 840 K, nekatere izopletne krivulje ter projekcije tekočinsko trdnih površin. Trdne raztopine kristalizirajo v Tl_5Te_3 kristalnem sistemu pri temperaturah strjavanja in nižjih.